

Seismicity at Intersections of Spreading Centers and Transform Faults

HUGH ROWLETT¹*Department of Geological Sciences, Brown University, Providence, Rhode Island 02912*

Ocean-bottom seismographs were used in a microearthquake monitoring experiment at the eastern junction of the Oceanographer transform with the mid-Atlantic ridge at 35°N. Microearthquake activity at the junction occurred over a broad area (>7 km). These microearthquakes 'cut across' the corner between the transform and median valley and are associated with fault scarps that form the inner walls on the west and north sides of the median and transform valleys. At intersections of other major fracture zones (>100-km offset) and slow to moderate spreading centers microearthquake activity is also diffuse and cuts across the corner between the spreading center and transform fault. The narrow zone of decoupling (~1 km) observed between spreading center and transform boundaries by detailed geological studies at the Tamayo/East Pacific Rise and Vema/mid-Atlantic Ridge intersections suggest that the diffuse seismicity (20 to 30 km in width) does not reflect a diffuse plate boundary at the transition from rift to transform valley. Instead, the faulting probably reflects internal deformation of the corner by secondary faults off of the plate boundary.

INTRODUCTION

Ocean-bottom seismographs (OBS's) were deployed at the eastern intersection of the Oceanographer transform with the mid-Atlantic ridge to study the transition from a spreading center to a transform fault. Studies of other transform/spreading center intersections show that microearthquake activity in the fracture zone does not extend past the spreading centers which are offset by the transform fault [Reid and Macdonald, 1973; Reid, 1976; Francis *et al.*, 1978; Forsyth and Rowlett, 1979; Project ROSE Scientists, 1980]. Seismicity studies at intersections of major transforms (ridge/ridge offsets >100 km) and spreading centers suggest that the fault pattern is complex [Prothero *et al.*, 1976; Francis *et al.*, 1978; Forsyth and Rowlett, 1979] and that microearthquakes are distributed over a wide zone. In contrast, detailed geological studies suggest that the locus of a narrow zone of transform faulting may extend to within 1 km of the spreading center [RISE Scientific Team, 1979; Forsyth and Rowlett, 1979].

The object of this paper is to present observations of the seismicity at the eastern intersection of the Oceanographer fracture zone and the mid-Atlantic ridge (MAR). Although the observations were limited by logistical problems and represent a reconnaissance study for future work, the distribution of microearthquakes with respect to major morphological features is similar to microearthquake distributions found at other spreading center/transform intersections. The second part of this paper discusses the relationship between microearthquakes and the existing geologic observations of surface faulting at intersections. It is suggested that secondary structures on the corner of the plate between the spreading center and transform may play an important role in the deformation of the lithospheric plate at intersections.

MICROEARTHQUAKE SURVEY

In November 1974, two OBS's were deployed from the R/V *Vema* as receivers in a refraction experiment and a microearthquake monitoring experiment (Figure 1). Figure 2 shows the positions of the OBS's with respect to the median valley and the transform. OBS 1 was deployed about 12 km west of

the median valley in the central valley of the transform. OBS 3 was deployed 9.7 km ENE of OBS 1. Reflection profiles and precision depth recordings (3.5 kHz) taken from several *Vema* cruises in the vicinity of the deployments show that the bottom is extremely rough, with little or no sediment cover.

OBS units used in this experiment were equipped with a hydrophone and two geophones (horizontal and vertical). These instruments are discussed in more detail by McDonald *et al.* [1977]. Although OBS 1 operated properly, recording signals from seismic refraction profiles and microearthquakes, there were difficulties with OBS 3. The hydrophone channel of OBS 3 did not record any data, and ground waves recorded by the geophone channels from shots were too emergent to be picked reliably. The microearthquakes and water waves from shots, however, were satisfactorily recorded by OBS 3.

Seismicity

Both OBS units recorded continuously on the seafloor for about 5 days. OBS 3 recorded up to 111 microearthquakes during 129 hours on the bottom; OBS 1 recorded 75 microearthquakes in 110 hours. Only 20 of these events were large enough to be recorded by both instruments. Two of the largest events were from the central portion of the transform, 70 to 90 km away. The smaller events recorded by one instrument apparently occurred near each of the instruments. Figure 3 summarizes the number of events recorded by both OBS's during the 5 days. With the exception of two short pulses in activity near OBS 3, seismicity near both OBS's was similar with an average of 15 to 20 events per day.

The rate of seismicity is between rates of about 10 events per day observed by Reid and Macdonald [1973] and 36 events per day by Spindel *et al.* [1974] near the FAMOUS area at 37°N on the MAR. Francis *et al.* [1977] point out, however, that the level of seismicity near the FAMOUS area can vary during a few months as much as 2 orders of magnitude along adjacent transform faults. Thus the level of activity during the short recording interval of this study may not be representative of the long-term activity at the junction of the Oceanographer fracture zone.

Location of Microearthquakes

To locate microearthquakes from a two-station array, assumptions about the velocity structure of the crust and the focal depths are necessary, and a choice between two ambiguous solutions must be made. The refraction results [Rowlett,

¹ Present address: Gulf Research and Development Company, P. O. Drawer 2038, Pittsburgh, Pennsylvania 15230.

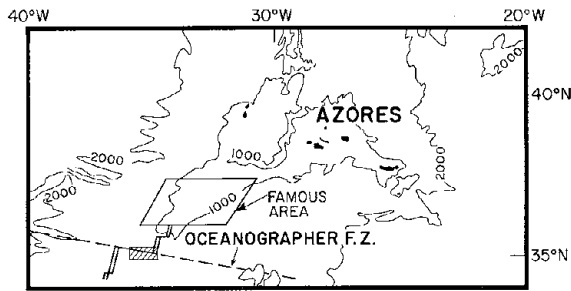


Fig. 1. Location map of study area on the mid-Atlantic ridge and the FAMOUS area. Hatched box is the area of the OBS experiment. Depth in meters, after Fox *et al.* [1979].

1978] suggest that 5.6 km/s is the dominant crustal velocity in the central valley of the transform. Therefore ranges from the OBS's to the microearthquakes are computed assuming a half-space model with a $V_p = 5.6$ km/s and $V_s = V_p/1.73$. Focal depths of individual events were varied from zero to the maximum depth permitted by S minus P times and the station separation. These assumptions are adequate, since epicenters calculated from the data set, using a range of reasonable values for V_p and focal depth, do not change the conclusions of this study.

Seven microearthquakes are located this way using both P and S phases picked on either the geophone or hydrophone channels. In Figure 4 the seismogram of a microearthquake is presented as an example of observed phases. The located events have S minus P times between 1.10 s and 2.83 s. There is, however, an ambiguity in the locations; that is, the microearthquakes can be located on either side of a line through the two OBS stations. Figure 2 shows epicentral locations of the microearthquakes at zero focal depth with respect to the basement contours and the OBS positions. The two possible locations (solid and open circles) for each of the microearthquakes are plotted in Figure 2. Note that regardless of the choice of epicentral location for each microearthquake, seismic activity near the junction of the median valley with the transform valley occurs over an area several kilometers wide, since in addition to the seven located events, there is also considerable seismic activity in the immediate vicinity of each OBS. That is, microearthquakes occur over an area at least 7 km wide, if all the microearthquakes were located on one side of the array (all solid or all opened circles), or over an area up to 14 km

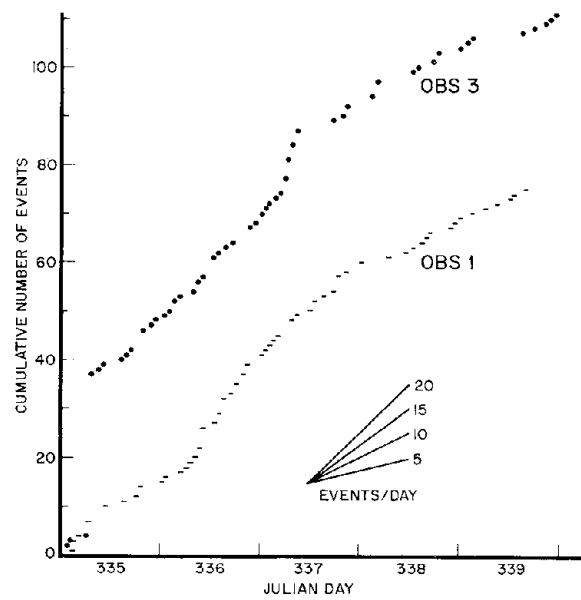


Fig. 3. Plot of the cumulative number of events recorded by OBS 1 and OBS 3 near the intersection of the Oceanographer transform with the northern rift axis. The event rate is about 15 to 20 events per day.

wide, if microearthquakes were located on both sides of the array (solid and opened circles).

If the bathymetry is known, the ambiguity in epicentral locations can be resolved using the additional information given by the travel time differences of the R_1 and P phases ($R_1 - P$). (The phase R_1 is a compressional phase that is a water wave multiple of P . See Figure 4.) Francis *et al.* [1977] also use ($R_1 - P$) times to locate microearthquakes recorded by an array of two OBS's. The method used differs from that of Francis *et al.*, since there is control on the crustal structure.

Because the ray path for R_1 crosses the seafloor about 2 km from an OBS (for reasonable crustal models), the velocity structure near the OBS has the greater effect on ($R_1 - P$) times than the structure near the source. Thus a velocity model of the central transform valley near OBS 1 is used to test for locations of the events. The crustal model consists of a 3.0-km/s layer, 1 km thick, over a 5.6-km/s refractor dipping 2° towards the east [Rowlett, 1978]. The main refractor (the bound-

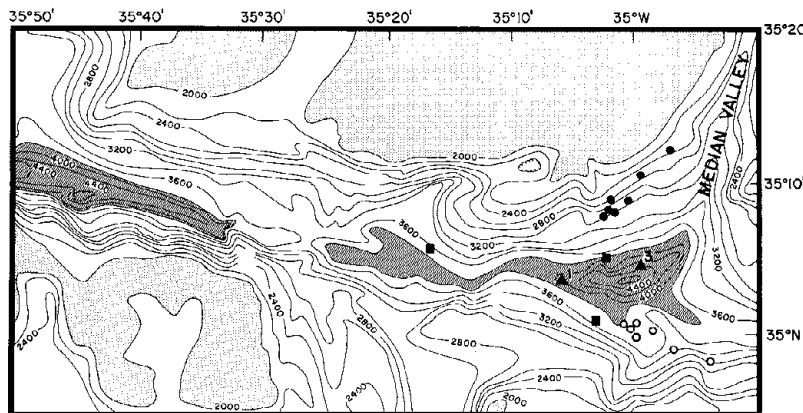


Fig. 2. Basement contours of eastern part of Oceanographer transform fault adapted from Schroeder *et al.* [1977] along with OBS positions (triangles), satellite fixes used to locate OBS positions (squares), preferred (solid circles) and alternative (open circles) locations of microearthquake epicenters. Choices of epicentral locations are explained in text.

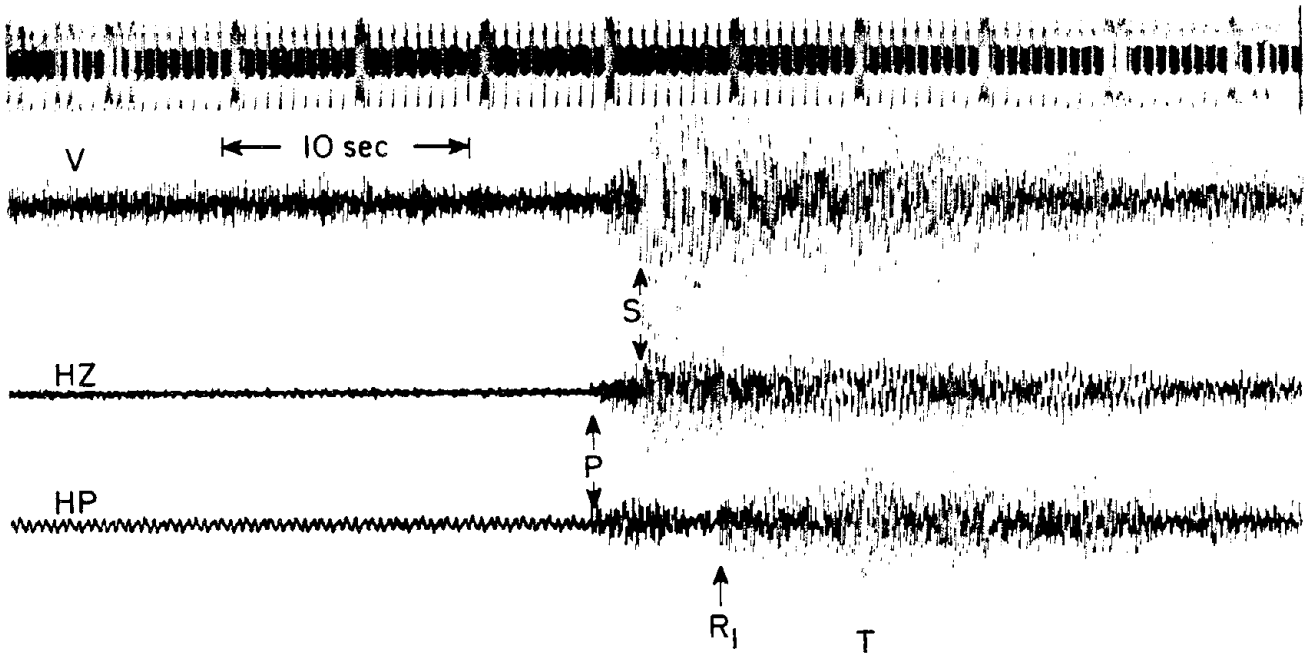


Fig. 4. Example seismogram of microearthquake recorded at OBS 1. The vertical, horizontal, and hydrophone traces are denoted by V, HZ, and HP, respectively. The same nomenclature is used for identifying phases as Francis and Porter [1973]. The noise on the HP trace is a result of the playback electronics. Event at 0205 GMT on day 337.

ary of the half space) of the crustal model is assumed to be a plane in three dimensions near OBS 1. Apparent dip of the main refractor is varied to compute ($R_1 - P$) times for events from different directions.

The ($R_1 - P$) times are calculated for sources located at depths above and below the main refractor. In cases where the refractor dips away from the OBS, ($R_1 - P$) times are equal to or greater than 5.13 s. The observed ($R_1 - P$) times for the seven events are between 4.91 and 5.05 s. Only cases with refractors that dip towards the OBS satisfy the observed ($R_1 - P$) times. Travel times of first arrivals from shots fired across the south wall of the transform valley require (if the refractions from these shots propagate along the same refractor derived for the velocity model beneath OBS 1) that the refractor beneath OBS 1 dips toward the southeast [Rowlett, 1978]. Epicenters southeast of OBS 1 cannot satisfy the observed ($R_1 - P$) times; therefore all of the epicenters are located north of the OBS array (solid circles in Figure 2). These results are

consistent with observations of seismicity at other intersections (see below).

In Figure 5, epicentral positions north of the OBS array are plotted for zero focal depth (solid circles) and for the maximum focal depth permitted by the S minus P times and the station separation (crosses). The maximum focal depths ranged between 6 and 12 km. Note that regardless of the focal depth the epicenters are located in an area where the west wall of the median valley (MV) bends around to form the north wall of the transform valley (TV). Schroeder [1977] analyzed surface-ship data over the Oceanographer fracture zone and suggested that major fault scarps form the inner wall west of the median valley and the wall north of the transform valley. He also suggested that the strike of the scarps along the western walls of the median valley bend around (approximating the contours in Figure 5) as the intersection with the transform valley is approached. The strikes of bathymetric contours begin to deviate from the general N20°E trend of the

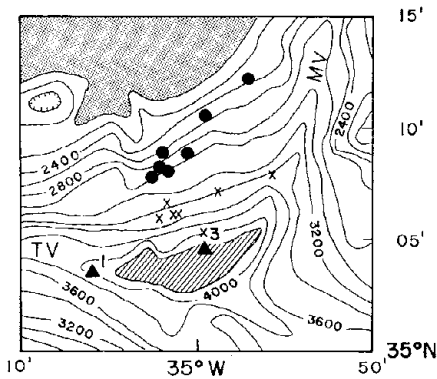


Fig. 5. Trade-off of epicentral position with depth. Epicenters at zero focal depth are denoted by dots, and epicenters at the maximum permitted focal depth are denoted by crosses. Bathymetry and symbols are the same as in Figure 2.

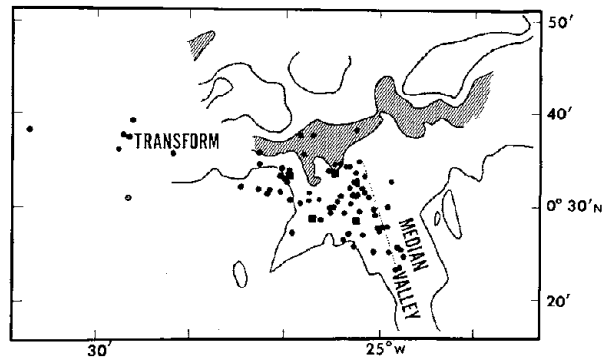


Fig. 6. Map of epicenters (dots) at the eastern intersection of St. Paul's transform and MAR [after Francis et al., 1978]. Squares denote OBS's. Dotted line denotes axis of median valley [from Francis, 1977]. Depths greater than 2300 fm (4206 m) and less than 1900 fm (3475 m) are hatched and stippled, respectively.

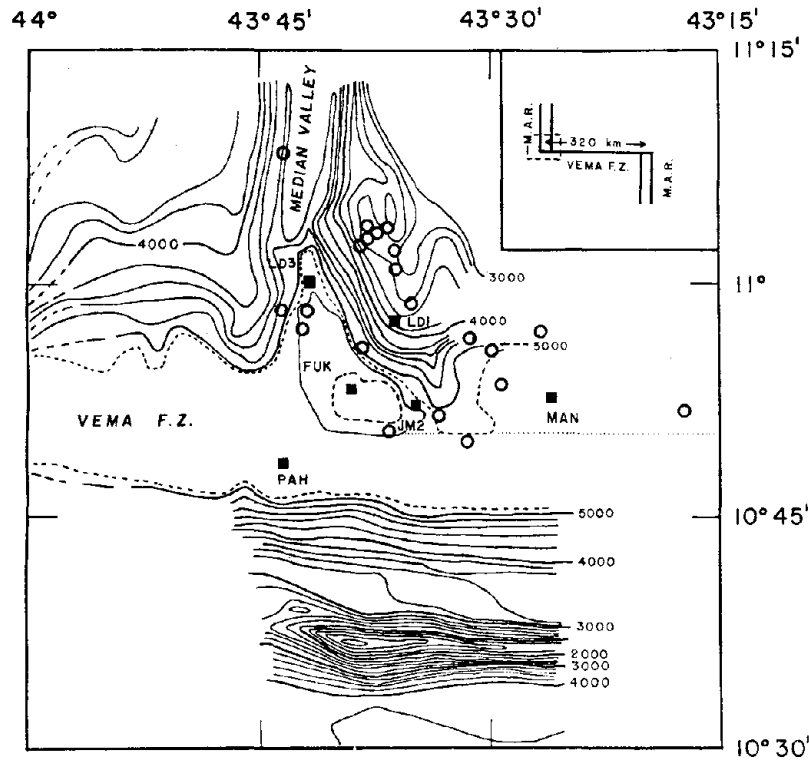


Fig. 7. Seismicity at the western intersection of the Vema transform (preliminary results of Forsyth and Rowlett [1979]). Open circles and squares represent microearthquakes and OBS's, respectively. Bathymetry in meters. Dotted line represents trace of transform fault.

median valley 25 to 30 km from the axis of the transform valley. The microearthquake locations suggest therefore that these oblique structures are presently active features.

Even with the limited recording interval of 5 days, it may be significant that a simple transform fault parallel to the east-west spreading direction at this latitude [Macdonald, 1977; Schroeder, 1977] is not delineated by the larger events at the intersection. It is possible that microearthquakes occurring near the instruments, but too small to be recorded by both instruments, represent simple transform faulting. Faulting away from the intersection and within the transform, however, is nearly parallel to the present spreading direction. The focal mechanisms of two teleseismic events clearly show strike-slip faulting with east-west slip vectors [Sykes, 1967; Rowlett, 1978].

FEATURES OF SEISMICITY AT INTERSECTIONS

A number of microearthquake surveys have been conducted with sonobuoy or OBS arrays at intersections of other major transforms [Reid, 1976; Prothero et al., 1976; Francis et al., 1978; Jones and Johnson, 1978; Forsyth and Rowlett, 1979; Project ROSE Scientists, 1980]. With the exception of the ROSE study, small arrays were used with resulting limitations in epicentral capabilities and with generally poor focal depth resolution. Nevertheless, taken together, these studies show features of the seismicity that are remarkably similar and thus may be characteristic of most intersections.

Figures 6-8 illustrate epicenters located at intersections of the St. Paul's, Vema, and Rivera fracture zones [from Francis et al., 1978; Forsyth and Rowlett, 1979; Reid, 1976]. At all of these intersections the microearthquakes occupy a triangular zone in the corner between the spreading axis and the trans-

form. This distribution of microearthquakes is similar to results at the intersection of the Oceanographer fracture zone. Microearthquake activity at the eastern intersection of the Blanco fracture zone may also occur at the corner between the spreading axis and transform. Measurements of the direction of approach of events recorded by a sonobuoy array positioned over the eastern intersection of the Blanco fracture zone indicate that most events were from the western crestal mountains of the northern Gorda Ridge [Jones and Johnson, 1978].

There is very little or no seismic activity in the corner between the spreading center and the inactive portion of the fracture zone (Figures 6-8). Seismic activity also appears limited to the young side of the transform valley at the Vema, St. Paul's, Rivera, and Oceanographer fracture zones (Figures 5-8). Because of array limitations the lateral extent of activity either along the transform or into the plate adjacent to the spreading center is unknown. In the case of the Vema transform, where deformed sediments in the transform valley provide a good indication of the transform fault [Eittreim and Ewing, 1975], the lateral extent of the diffuse zone of microearthquake activity appears limited by the transform fault itself (Figure 7 and Forsyth and Rowlett [1979]). Forsyth and Rowlett [1979] observed disturbances in sediments at the Vema fracture zone that indicate vertical displacement on the spreading center/transform corner north of the transform stops abruptly at the active transform trace. This abrupt boundary is not surprising because large, lateral differences in physical properties of the lithosphere probably exist across major transforms near their intersections where hot, thin lithosphere is adjacent to cooler and thicker lithosphere [Parker and Oldenburg, 1973; Loudon and Forsyth, 1976; Rowlett and Forsyth, 1979].

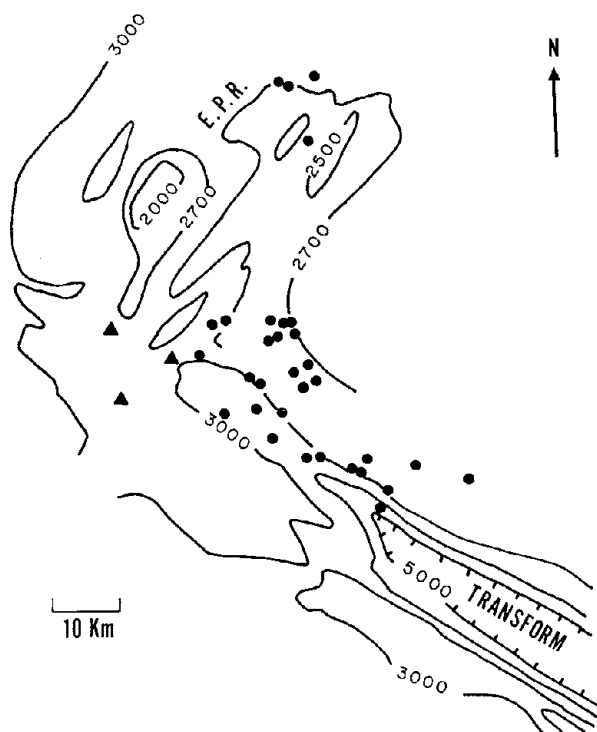


Fig. 8. Microearthquakes (dots) at the western intersection of the Rivera transform with the EPR [after Reid, 1976]. Bathymetry in meters. Triangles denote OBS's.

The distribution of microearthquakes at the western intersection of the Orozco fracture zone and the East Pacific Rise (at $15^{\circ}15'N$) is different from the examples mentioned above. Microearthquakes lie within the active transform along a narrow trough that extends eastward from the intersection with the northern rise crest [Project ROSE Scientists, 1980]. There is little or no activity in the western corner between the spreading center and transform fault.

The spreading rates of the spreading centers adjacent to the intersections considered here vary from 1.1 cm/yr near the Oceanographer fracture zone to 4.9 cm/yr near the Orozco fracture zone. That is, the adjacent spreading centers are characterized by slow to fast spreading rates. The difference between the distribution of seismicity at the intersections of the Orozco fracture zone and the other fracture zones considered here may be a function of spreading rates. Other features of intersections are also known to be functions of spreading rates. For example, Macdonald *et al.* [1979] suggest for spreading rates greater than 4 cm/yr that the spreading center near the intersection is not characterized by an 'intersection rift' (or depression) that characterizes intersections at slower spreading rates. Likewise, Atwater and Macdonald [1977] found that transform/spreading intersections were oblique for spreading rates less than 2 cm/yr, orthogonal for rates greater than 4 cm/yr, and either oblique or orthogonal at intermediate spreading rates.

DISCUSSION AND CONCLUSIONS

The seismicity at intersections of transforms and slow to moderate spreading centers is concentrated on the corner of the plate between the spreading center and transform. This seismicity probably reflects a gradual transition between extensional and transform structures. Bathymetry at inter-

sections of the Oceanographer, St. Paul's, Vema, Rivera, Blanco, and Tamayo fracture zones also suggest interaction between the spreading center and transform fault. For example, near these intersections, bathymetric contours parallel to the spreading center change trend and bend around at the seismically active corner of the plate near the transform (Figures 5-8; Figure 1 of Jones and Johnson [1978]; Figure 2 of Macdonald *et al.* [1979]). Bathymetric contours on the seismically inactive corner between the spreading center and the inactive portion of the fracture zone are generally parallel to the spreading center and do not change trend near the fracture zone.

Interpretation of the seismicity at the intersection in terms of a broad plate boundary is not consistent with detailed surface-ship observations at the Vema intersection and the MAR [Forsyth and Rowlett, 1979] and with near-bottom observations at the Tamayo intersection with the EPR [RISE Scientific Team, 1979; Macdonald *et al.*, 1979]. These detailed observations show that the zone of active transform faulting apparently extends ~ 1 km from the spreading center and is very narrow (< 1 km wide). Thus the plate boundary is probably well defined at the intersection, and much of the microearthquake activity is concentrated off of the boundary and within the plate.

The actual causes and mechanisms of the deformation within the corner of the plate are unknown, since there have been no focal mechanism studies of the microearthquakes. Near-bottom observations of the geology at intersections, however, suggest one type of deformation that is consistent with the locations of the microearthquakes. Structures trending oblique to both the spreading center and transform are observed at several intersections with slow to moderate spreading centers [ARCYANA, 1975; Whitmarsh and Laughton, 1976; Searle and Laughton, 1977; Macdonald *et al.*, 1979]. These oblique structures appear to be fault scarps and may represent strains of limited extent caused by transform motion on newly created oceanic crust [Searle and Laughton, 1977; Macdonald *et al.*, 1979]. Whitmarsh and Laughton [1976] show that the oblique features are associated with only the spreading center/transform corner and not with the other corner. This restriction of the oblique structures to one corner is the same as the location of seismic activity at intersections and offers an explanation for the type of faulting causing the diffuse seismicity at intersections of slow to moderate spreading centers.

Acknowledgments. I am grateful to F. Schroeder for providing bathymetric charts prior to publication and P. Fox for a preprint. O. Perez contributed to the analysis of data from the Oceanographer fracture zone. I thank H. Kohler and the officers and crew of the R/V *Vema* for their valuable assistance. Special thanks go to W. Macdonald, R. Bookbinder, G. Gunther, and A. Hubbard for the work with the OBS's at the Oceanographer fracture zone. D. W. Forsyth provided many stimulating discussions and ideas. This study was supported under grants from the National Science Foundation, NSF DES74-24698, NSF OCE76-82058, and NSF OCE79-09404 and the Office of Naval Research grant N00014-76-0818. Lamont-Doherty Geological Observatory contribution 3077.

REFERENCES

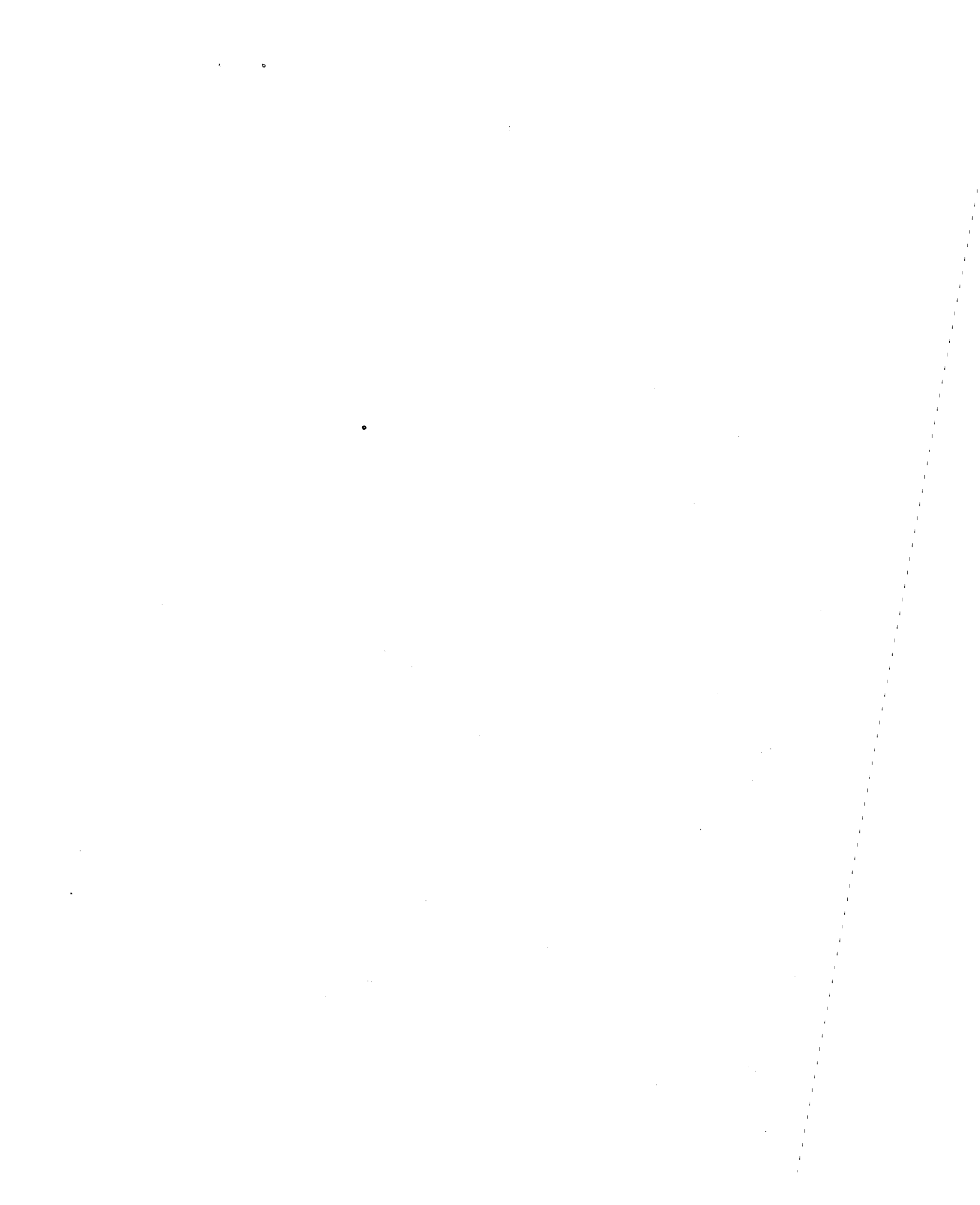
- ARCYANA, Transform fault and rift valley from bathyscaph and diving saucer, *Science*, 190, 108-116, 1975.
 Atwater, T., and K. C. Macdonald, Are spreading centers perpendicular to their transform faults?, *Nature*, 270, 715-719, 1977.

- Eittrheim, S., and J. Ewing, Vema fracture zone transform fault, *Geology*, 3, 555-558, 1975.
- Forsyth, D., and H. Rowlett, Microearthquakes and recent faulting at the intersection of the Vema fracture zone and the Mid-Atlantic ridge (abstract), *Eos Trans. AGU*, 60, 376, 1979.
- Fox, P. J., F. W. Schroeder, R. M. Moody, W. C. Pitman III, and P. J. Hoose, The bathymetry of the Oceanographer Fracture Zone and mid-Atlantic ridge at 35°N with implications for central North Atlantic plate motion, *Mar. Geol.*, 1979.
- Francis, T. J. G., A bathymetric survey of the eastern end of the St. Paul's Fracture Zone, in Voyage of Discovery, *Deep Sea Res.*, 24, supplement, 637-645, 1977.
- Francis, T. J. G., and I. T. Porter, Median valley seismology: Mid-Atlantic ridge near 45°N, *Geophys. J. R. Astron. Soc.*, 43, 279-311, 1973.
- Francis, T. J. G., I. T. Porter, and J. R. McGrath, Ocean-bottom seismograph observations on the mid-Atlantic ridge near lat. 37°N, *Geol. Soc. Am. Bull.*, 88, 644-677, 1977.
- Francis, T. J. G., I. T. Porter, and R. C. Lilwall, Microearthquakes near the eastern end of St. Paul's Fracture Zone, *Geophys. J. R. Astron. Soc.*, 53, 201-217, 1978.
- Jones, P. R., and S. H. Johnson, Sonobuoy array measurements of active faulting on the Gorda Ridge, *J. Geophys. Res.*, 83, 3435-3440, 1978.
- Louden, K. E., and D. W. Forsyth, Thermal conduction across fracture zones and the gravitational edge effect, *J. Geophys. Res.*, 81, 4869-4874, 1976.
- Macdonald, K. C., Near-bottom magnetic anomalies, asymmetric spreading, oblique spreading and tectonics of the mid-Atlantic ridge near lat. 37°N, *Geol. Soc. Am. Bull.*, 88, 541-555, 1977.
- Macdonald, K. C., K. Kastens, F. N. Spiess, and S. P. Miller, Deep tow studies of the Tamayo transform fault, *Mar. Geophys. Res.*, 4, 37-70, 1979.
- McDonald, W. G., A. C. Hubbard, R. G. Bookbinder, and K. McCamy, Design and shipboard operation of a multipurpose ocean bottom seismograph, *Mar. Geophys. Res.*, 3, 179-196, 1977.
- Parker, R. L., and D. W. Oldenburg, Thermal model of ocean ridges, *Nature Phys. Sci.*, 242, 137-139, 1973.
- Project ROSE Scientists, Seismicity of the Orozco fracture zone: Overview of the passive phase of ROSE, *Eos Trans. AGU*, 61, 288, 1980.
- Prothero, W. A., I. Reid, M. S. Reichle, and J. N. Brune, Ocean bottom seismic measurements on the East Pacific Rise and Rivera Fracture Zone, *Nature*, 262, 121-124, 1976.
- Reid, I., The Rivera plate: A study in seismology and plate tectonics, Ph.D. thesis, 288 pp., Univ. of Calif., San Diego, 1976.
- Reid, I., and K. Macdonald, Microearthquake study of the mid-Atlantic ridge near 37°N using sonobuoys, *Nature*, 246, 88-90, 1973.
- RISE Scientific Team, The Tamayo Transform: Insight into the tectonic behavior of ridge/ridge transform fault boundaries (abstract), *Eos Trans. AGU*, 60, 376-377, 1979.
- Rowlett, H., Seismic and tectonic studies of plate boundaries: Mid-Atlantic ridge at 37°N, Oceanographer fracture zone and margin of the Philippine Sea plate, Ph.D. thesis, 147 pp., Columbia Univ., New York, 1978.
- Rowlett, H., and D. Forsyth, Teleseismic P-wave delay times in a major oceanic fracture zone, *Geophys. Res. Lett.*, 6, 273-276, 1979.
- Schroeder, F. W., A geophysical investigation of the Oceanographer fracture zone and the mid-Atlantic ridge in the vicinity of 35°N, Ph.D. thesis, 229 pp., Columbia Univ., New York, 1977.
- Searle, R. C., and A. S. Laughton, Sonar studies of the mid-Atlantic ridge and Kurchatov fracture zone, *J. Geophys. Res.*, 82, 5313-5328, 1977.
- Spindel, R. C., S. B. Davis, K. C. Macdonald, R. P. Porter, and J. D. Phillips, Microearthquake survey of median valley of the mid-Atlantic ridge at 36°30'N, *Nature*, 248, 577-579, 1974.
- Sykes, L. R., Mechanism of earthquakes and nature of faulting on the mid-Atlantic ridge, *J. Geophys. Res.*, 72, 2131-2153, 1967.
- Whitmarsh, R. B., and A. S. Laughton, A long-range sonar study of the mid-Atlantic ridge crest near 37°N (FAMOUS area) and its tectonic implications, *Deep Sea Res.*, 23, 1005-1023, 1976.

(Received August 20, 1979;
revised October 2, 1980;
accepted October 13, 1980.)

Accession For	
NTIS GRA&I	<input checked="" type="checkbox"/>
DTIC TAB	<input type="checkbox"/>
Unannounced	<input type="checkbox"/>
Justification	
By	
Distribution/	
Availability Codes	
Dist	Avail and, or Special
A	20

SDTIC
ELECTE
JUL 06 1981
D





REPORT DOCUMENTATION PAGE		READ INSTRUCTIONS BEFORE COMPLETING FORM
1. REPORT NUMBER	2. GOVT ACCESSION NO. AD-A100 943	3. RECIPIENT'S CATALOG NUMBER
4. TITLE (and Subtitle) Seismicity at Intersections of Spreading Centers and Transform Faults		5. TYPE OF REPORT & PERIOD COVERED Journal article
		6. PERFORMING ORG. REPORT NUMBER LDGO NO. 3077
7. AUTHOR(s) Hugh Rowlett		8. CONTRACT OR GRANT NUMBER(s) N00014-76-0818
9. PERFORMING ORGANIZATION NAME AND ADDRESS Lamont-Doherty Geological Observatory of Columbia University Palisades, NY 10964		10. PROGRAM ELEMENT, PROJECT, TASK AREA & WORK UNIT NUMBERS Task Order No. Nr. 083-142
11. CONTROLLING OFFICE NAME AND ADDRESS Dept. of The Navy Code 480, Office of Naval Research Arlington, Virginia 22217		12. REPORT DATE June 25, 1981
		13. NUMBER OF PAGES 6
14. MONITORING AGENCY NAME & ADDRESS (if different from Controlling Office)		15. SECURITY CLASS. (of this report) Unclassified
		15a. DECLASSIFICATION/DOWNGRADING SCHEDULE
16. DISTRIBUTION STATEMENT (of this Report) Approved for public release; distribution unlimited		
17. DISTRIBUTION STATEMENT (of the abstract entered in Block 20, if different from Report)		
18. SUPPLEMENTARY NOTES Reprinted from Journal of Geophysical Research Vol. 86, No. B5, pp 3815 - 3820, May, 1981.		
19. KEY WORDS (Continue on reverse side if necessary and identify by block number) Seismicity Spreading Centers Transform Faults		
20. ABSTRACT (Continue on reverse side if necessary and identify by block number) Ocean-bottom seismographs were used in a microearthquake monitoring experiment at the eastern junction of the Oceanographer transform with the mid-Atlantic ridge at 35°N. Microearthquake activity at the junction occurred over a broad area (>7 km). These microearthquakes 'cut across' the corner between the transform and median valley and are associated with fault scarps that form the inner walls on the west and north sides of the median and transform valleys. At intersections of other major fracture zones (>100-km offset) and slow to moderate spreading centers microearthquake activity is also diffuse and cuts across the corner between the spreading center and transform fault. The narrow zone of decoupling (~1 km) observed between spreading center and transform boundaries by detailed geological		

Unclassified

SECURITY CLASSIFICATION OF THIS PAGE (When Data Entered)

(20. continued)

studies at the Tamayo/East Pacific Rise and Vema/mid-Atlantic Ridge intersections suggest that the diffuse seismicity (20 to 30 km in width) does not reflect a diffuse plate boundary at the transition from rift to transform valley. Instead, the faulting probably reflects internal deformation of the corner by secondary faults off of the plate boundary.

Unclassified

SECURITY CLASSIFICATION OF THIS PAGE(When Data Entered)